Available online at www.sciencedirect.com
SCIENCE DIRECT®
Journal of Nuclear Materials 352 (2006) 6–12
journal of nuclear materials
www.elsevier.com/locate/jnucmat

Optical characterization of tristructural isotropic fuel particle cross-sections using generalized ellipsometry

G.E. Jellison Jr. *, J.D. Hunn, R.A. Lowden

Materials Science and Technology Division, Oak Ridge National Laboratory, Oak Ridge, TN 37831-6030, United States

Abstract

One particularly important measure of quality of tristructural isotropic (TRISO) fuel particles is the degree of preferred orientation of crystallites in the polycrystalline pyrolytic carbon coatings. Excessive crystallographic anisotropy leads to unwanted anisotropic dimensional changes during irradiation that can cause the TRISO coatings to fail. Early optical methods were developed in the 60s and 70s to measure this anisotropy by taking advantage of the large optical anisotropy of graphite. Since that time, there have been significant improvements in both the theoretical understanding and experimental techniques in the understanding of optical anisotropy. Here we discuss a new method, based on the two-modulator generalized ellipsometer (2-MGE) to measure the optical anisotropy. This technique has been demonstrated to measure the optical diattenuation to an accuracy from ± 0.001 to ± 0.005 and the preferred direction of the crystallites to an accuracy of better than $\pm 2°$ with a spatial resolution of better than 5 μm. Diattenuation 'pictures' of the nuclear fuel cross-sections reveal that the inner pyrocarbon layer (IPyC) is far from uniform both in the degree of diattenuation and in the direction of the principal axis. The 2-MGE technique is faster, more accurate, and collects considerably more data than previous optical anisotropy measurements of TRISO fuel particles.

1. Introduction

It has been known for a long time that polarized light reflected from nanocrystalline graphite is sensitive to the crystallographic anisotropy of the crystallites. If the nanocrystallites are randomly oriented, then there is no polarization dependence on the reflected light. However, nanocrystalline graphite can become crystallographically semi-aligned in micron-sized regions of the material, resulting in a polarization-dependent reflectivity of the material. Using microscopy, it is possible to obtain 'maps' of these regions.

Excessive crystallographic anisotropy leads to anisotropic dimensional changes in pyrolytic carbon during irradiation. In TRISO-coated fuel particles, anisotropic dimensional changes in the inner pyrolytic carbon (IPyC) layer can result in coating failure. For this reason, quantification of this preferred orientation of crystallites in the IPyC layer has become an important measurement for quality control, which is normally done using optical reflection of polarized light.

Optically, graphite is a uniaxial semi-metallic material, requiring two values of the refractive index n and two values of the extinction coefficient k to

* Corresponding author. Tel.: +1 865 576 7309; fax: +1 865 574 4143.
E-mail address: jellisongejr@ornl.gov (G.E. Jellison Jr.).

0022-3115/$ - see front matter © 2006 Elsevier B.V. All rights reserved.
doi:10.1016/j.jnucmat.2006.02.081

describe the optical response at each wavelength. The ordinary values n_o and k_o are related to the optical response for light polarized perpendicular to the optic axis (the c-axis), while the extraordinary values n_e and k_e are related to the optical response for light polarized parallel to the optic axis. Because of its highly anisotropic crystal structure, it is expected that the extraordinary values will be considerably different from the ordinary values. The ordinary optical functions of graphite (n_o and k_o) are reasonably well-known, but there is significant uncertainty in the extraordinary optical functions of graphite (n_e and k_e) [1,2].

In this paper, we will discuss a new approach to the measurement of the optical anisotropy of pyrocarbon utilizing a variant of the two-modulator generalized ellipsometer (2-MGE) [3–5]. We will show that this approach yields considerably more information in less time than older techniques, and this new information has led to additional insight into potential defects in TRISO fuel.

2. The old way: optical anisotropy factor (OAF)

The simplest measurement of the Optical Anisotropy Factor (OAF) consists of two measurements with a microscope: one with the input beam polarized along the radius of the particle, the other with the input beam polarized perpendicular to this radius. The OAF is then defined as

$$\mathrm{OAF} = R_{\max}/R_{\min}, \tag{1}$$

where $R_{\max}(R_{\min})$ is the maximum (minimum) reflectivity. In some cases, there is an additional polarizer on the output beam. Typically, these measurements are made using light from a HeNe laser.

There are several potential problems with this approach. First of all, the technique only measures a single quantity, but the optical properties of graphite are so complicated that more parameters may be required. Second of all, the OAF measurements are done sequentially, so fluctuations in the light level or the position of the measured spot between the first and second measurements will result in error. Thirdly, light from a HeNe laser is coherent, resulting in intensity variations across the laser beam, particularly after traversing several optics (speckle). There is no way to normalize these errors out of the final value, dramatically increasing the final error in the value of the OAF.

3. The new way: generalized ellipsometry

Over the last 10 years, there has been a considerable improvement in the understanding of complicated polarization measurements. Older ellipsometric measurements were routinely used for the characterization of isotropic systems, but more complicated systems containing anisotropic materials required more sophisticated measurement techniques, often called generalized ellipsometry. Moreover, generalized ellipsometry measurements can be performed in different configurations from standard ellipsometry, such as in transmission or at normal-incidence reflection.

In transmission or normal-incidence reflection, the measured parameters have different meanings than they do in standard ellipsometric configurations. If it is assumed that the sample is uniaxial with the optic axis lying in the plane of the sample, then we can define two reflectances: R_o for light polarized perpendicular to the optic axis and R_e for light polarized parallel to the optic axis. The diattenuation N is defined as

$$N = \frac{R_e - R_o}{R_o + R_e}. \tag{2}$$

The diattenuation is a common parameter in polarization optics, and measures the degree of residual polarization of a light beam after interaction. If the optic totally linearly polarizes the beam, then $N = \pm 1$, while an isotropic optic results in $N = 0$. Clearly, the diattenuation N is related to the OAF by

$$\mathrm{OAF} = R_o/R_e = (1+N)/(1-N) \sim 1 + 2N, \tag{3}$$

where we have ignored the possible problems with signs, since this will depend upon sample orientation.

Similarly, a light beam reflecting from an anisotropic metallic surface will undergo a polarization-dependent phase shift, where the optical retardation $\delta = \phi_e - \phi_o$. This is quite different from the transmission ellipsometry case, where the optical retardation measures the accumulated phase change that one polarization state is retarded with respect to the other; for example, a quarter wave plate would have $\delta = \pi/2$.

To measure these parameters for TRISO fuel particles, we have used the two-modulator generalized ellipsometry microscope (2-MGEM), shown schematically in Fig. 1. The light source is a mercury lamp focused onto a tapered fiber. Light emitting from end of the fiber is collimated by the microscope

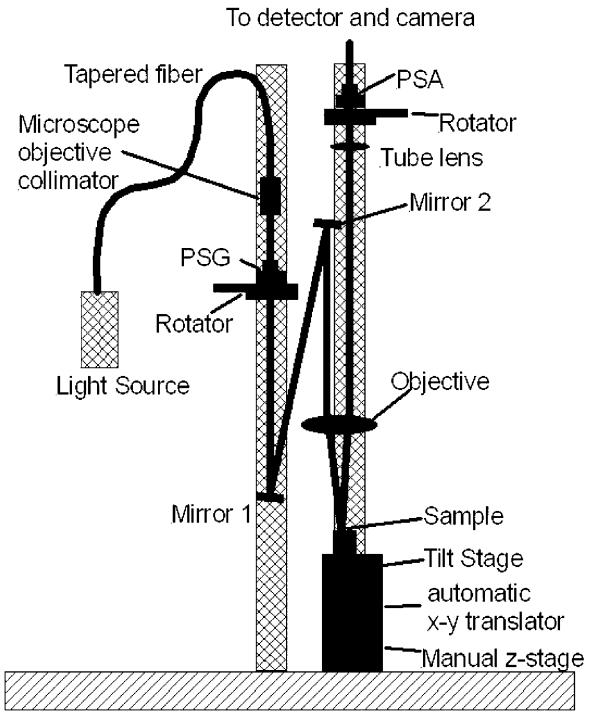

Fig. 1. Schematic diagram of the 2-MGEM.

objective before it passes through the polarization state generator (PSG), reflects off mirrors 1 and 2 to re-direct the light beam, and then is focused using the large diameter objective. Reflected light is imaged using the same objective and a tube lens onto a detector assembly (not shown), which can image the sample onto a CCD array and a pinhole in front of a photomultiplier tube (PMT). The Polarization state analyzer (PSA) is placed between the imaging optics and the detector assembly, and is used to characterize the polarization state of the reflected light. The light intensity waveform incident upon the PMT is analyzed to determine 8 parameters characteristic of the polarization-dependent reflective properties of the part of the sample imaged onto the pinhole. The wavelength is selected by placing an appropriate interference filter in front of the detector assembly; we normally use the 577 nm line of the mercury spectrum.

The polarization state of the PSG is dynamically elliptically polarized, cycling through linear, elliptical, and circular polarization states at the resonant frequency of the photoelastic modulator (PEM) (50 kHz in our case). Similarly, the reflected polarization state is cycled at the frequency of the PSA PEM (60 kHz in our case); see Refs. [2–6] for a more complete description. The resulting light intensity waveform can be simply expressed as

$$\begin{aligned}\text{Intensity}\ (t) = {} & I_{\mathrm{dc}} + I_{X0}X0 + I_{Y0}Y0 + I_{X1}X1 \\ & + I_{Y1}Y1 + I_{X0X1}X0X1 \\ & + I_{X0Y1}X0Y1 + I_{Y0X1}Y0X1 \\ & + I_{Y0Y1}Y0Y1. \end{aligned} \tag{4a}$$

The terms I_{dc}, I_{X0}, I_{Y0}, etc. are constants that multiply the basis functions:

$$X0 = \sin(A_0 \sin(\omega_0 t)); \quad Y0 = \cos(A_0 \sin(\omega_0 t)), \tag{4b, c}$$

$$X1 = \sin(A_1 \sin(\omega_1 t)); \quad Y1 = \cos(A_1 \sin(\omega_1 t)). \tag{4d, e}$$

These basis functions are not just Fourier basis functions, but rather sines and cosines of sines. The modulator amplitudes (A_0 and A_1) are measured in angular units (usually radians) and the modulator frequencies are given by ω_0 and ω_1. The intensity is normalized to the dc level, and this is done both in hardware and software. This has several advantages. First of all, the experiment is immune to fluctuations of the incident light beam, or in differences in sample reflection or transmission, assuming that enough light gets through to do the measurement; even 60 Hz noise can be eliminated. Second, the digitizing electronics are considerably simpler, since only one gain setting is needed. Thirdly, any light that does not get transmitted to the detector, whether it be absorbed in the sample or non-specularly reflected out of the collection cone of the optics, is lost, but does not contribute to systematic error of the experiment. This can be contrasted to any reflectivity measurement (such as the traditional OAF), where light lost due to non-specular reflection results in a systematic error. The 8 coefficients measured by the 2-MGEM are naturally very accurate, typically better than ± 0.001 for small values and ± 0.005 for values near ± 1.

The coefficients of the basis functions shown in Eq. (4a) are the parameters required for the measurement. If the PSG is set to 0° and the PDA is set to 45°, then the 8 parameters are:

$$I_{X0} = \mathrm{CD} \quad I_{X1} = -\mathrm{CD}, \tag{5a, b}$$

$$I_{Y0} = \sin(2\gamma)N \quad I_{Y1} = -\cos(2\gamma)N, \tag{5c, d}$$

$$I_{X0X1} = -C \quad I_{Y0X1} = -\cos(2\gamma)S, \tag{5e, f}$$

$$I_{X0Y1} = \sin(2\gamma)S \quad I_{Y0Y1} = \cos(2\gamma)\sin(2\gamma)(1 + C), \tag{5g, h}$$

where γ is the angle between the measurement system and the optic axis of the sample and the quantities S and C are given by $S = (1 - N^2)^{1/2} \sin(\delta)$ and by $C = (1 - N^2)^{1/2} \cos(\delta)$, where δ is the retardation. Obviously, N, S, and C are not independent, since $N^2 + S^2 + C^2 = 1$. (Note that depolarization is indicated if the sum $N^2 + S^2 + C^2 = \beta^2 < 1$.) The quantity CD in Eq. (5) is the circular diattenuation, which is normally close to zero.

One additional advantage for 2-MGE for microscopic applications is that the modulation is obtained by vibrating a crystal, not by rotating an optical element. Therefore, beam precession and registry are never an issue, since all 8 parameters are taken by definition on the same spot of the sample.

4. Sample results

The 2-MGEM data consists of an intensity value and 8 measured parameters (see Eq. (5)) and associated errors for each pixel measured. These data are then reduced to diattenuation N, direction of the principal axis γ, retardation δ, circular diattenuation CD, and polarization factor β. Clearly, each 'picture' can contain many megabytes of data, depending on the size and the resolution of the scan.

4.1. Rutile

As a first test of the 2-MGEM, a sample of single crystal rutile (TiO_2) with the optic axis in the sample surface plane was obtained from Commercial Crystal Laboratories, Inc. (Naples, Florida). 2-MGEM measurements were taken over a 0.5×0.5 mm area with a resolution of 0.005 mm ($101 \times 101 = 10\,201$ points). Averaged over all points, the average diattenuation and the associated standard deviation is $|N| = 0.0881 \pm 0.0011$. As a comparison, we calculated the diattenuation from the refractive indices of rutile determined from spectroscopic generalized ellipsometry measurements ($n_o = 2.628 \pm 0.002$, $n_e = 2.919 \pm 0.002$, $k_o = k_e = 0.0$) [7], and got 0.0870 ± 0.0008, indicating agreement between the two measurements. The direction of the principal axis was also determined to be $158.0 \pm 0.2°$, which indicates that the 2-MGEM can be used to determine the direction of the fast axis very accurately.

4.2. Highly oriented pyrolytic graphite

Highly oriented pyrolytic graphite (HOPG) is known to be the most highly oriented form of graphite, although it is not single crystal. Several samples of this material have been examined using the 2-MGEM, where the sample was cut and polished such that the c-axis lay in the sample surface plane. The average diattenuation observed at a wavelength of 633 nm is $|N| \sim 0.59$, $|S| \sim 0.25$, and $|C| \sim 0.79$. (Direct comparison with experimental values is not possible due to the inaccuracies of n_e and k_e.) The direction of the optic axis (principal axis) is perpendicular (parallel) to the graphine layers. Very little circular diattenuation is observed, except in regions a large transitions. All parameters are relatively constant over the sample, but there are regions of obvious defects where the local values are quite different from averages. In all cases, there is very little depolarization, indicating that the measurement is good even in regions of reduced intensity.

4.3. TRISO fuel

Fig. 2 shows an example of high-resolution 2-MGEM data (pixel size: 2 μm) taken on a surrogate particle. The kernel was ZrO_2 and three additional layers were deposited: buffer, inner pyrocarbon (IPyC), and silicon carbide (SiC). All coatings are applied using a fluidized bed CVD process. The IPyC layer was deposited using pure C_3H_6 to enhance the optical anisotropy. As can be seen from the figure, the intensity plot (Fig. 2(a)) clearly indicates the boundaries of the 3 layers, as well as several scratches and defects on the surface. Fig. 2(b) shows that the diattenuation of the IPyC is large and quite non-uniform. In addition, there is an observable diattenuation in the buffer layer, but the SiC layer shows no observable diattenuation. Fig. 3 shows an expanded view of the diattenuation of this particle Fig. 3(a), as well as similar regions taken from 2-MGEM data of similar particles, but where the IPyC was deposited using different coating mixtures (Fig. 3(b): C_2H_2:C_3H_6 = 1:2; Fig. 3(c): C_2H_2:C_3H_6 = 1:1); note that the scale of Fig. 3(a) is 0–0.06, while the scale for Fig. 3(b) and (c) is 0–0.02. In Fig. 3, the direction of the principal axis is superimposed on each color-coded pixel.

Fig. 4 shows an example of high-resolution 2-MGEM data taken on a polished cross-section of German TRISO Fuel [depleted uranium kernel, buffer, IPyC, SiC, outer pyrocarbon (OPyC)]. From the intensity plot (Fig. 4(a)), it is easy to see the kernel, buffer layer, IPyC layer, and the SiC layer. The OPyC layer is also present but is not obvious over

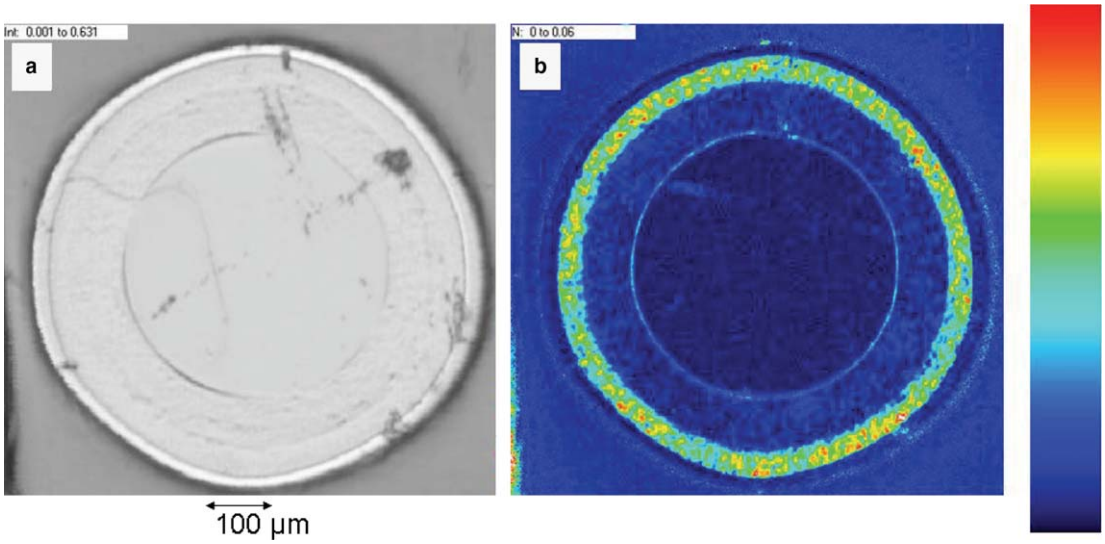

Fig. 2. 2-MGEM data from a surrogate particle with ZrO_2 kernel and 3 layers (buffer, IPyC, SiC), where the IPyC was grown using pure C_3H_6. The 2-MGEM data was taken using 2-μm pixel size. The intensity (a, on a log scale) and the diattenuation (b, 0–0.06). The scale to the right is also used for Figs. 3 and 4 where red is the scale maximum and black is the scale minimum.

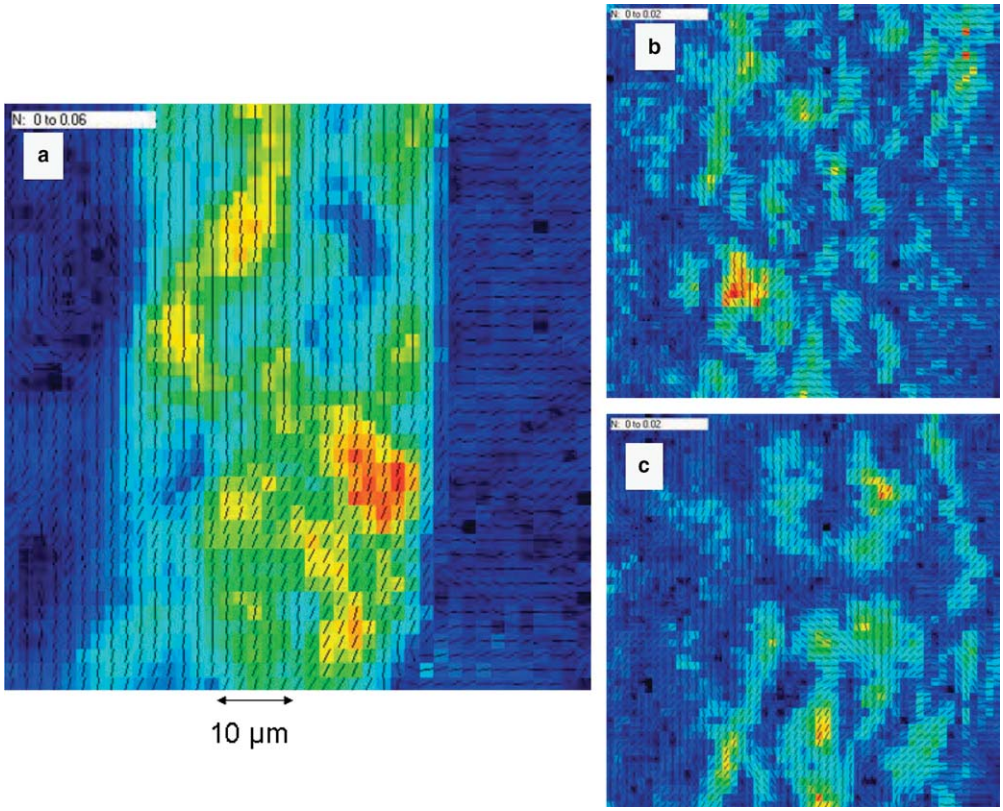

Fig. 3. 2-MGEM data of the IPyC of surrogate ZrO_2 particles with three layers (buffer, IPyC, SiC) at a pixel size of 2 microns. The IPyCs were grown using different pure C_3H_6 mixing ratios: (a, C_2H_2:C_3H_6 see Fig. 2; scale: 0–0.06); (b, 1:2, scale: 0–0.02); (c, 1:1, scale: 0–0.02). The lines drawn in the figure correspond to the direction of the principal axis. See Fig. 2 for the scale.

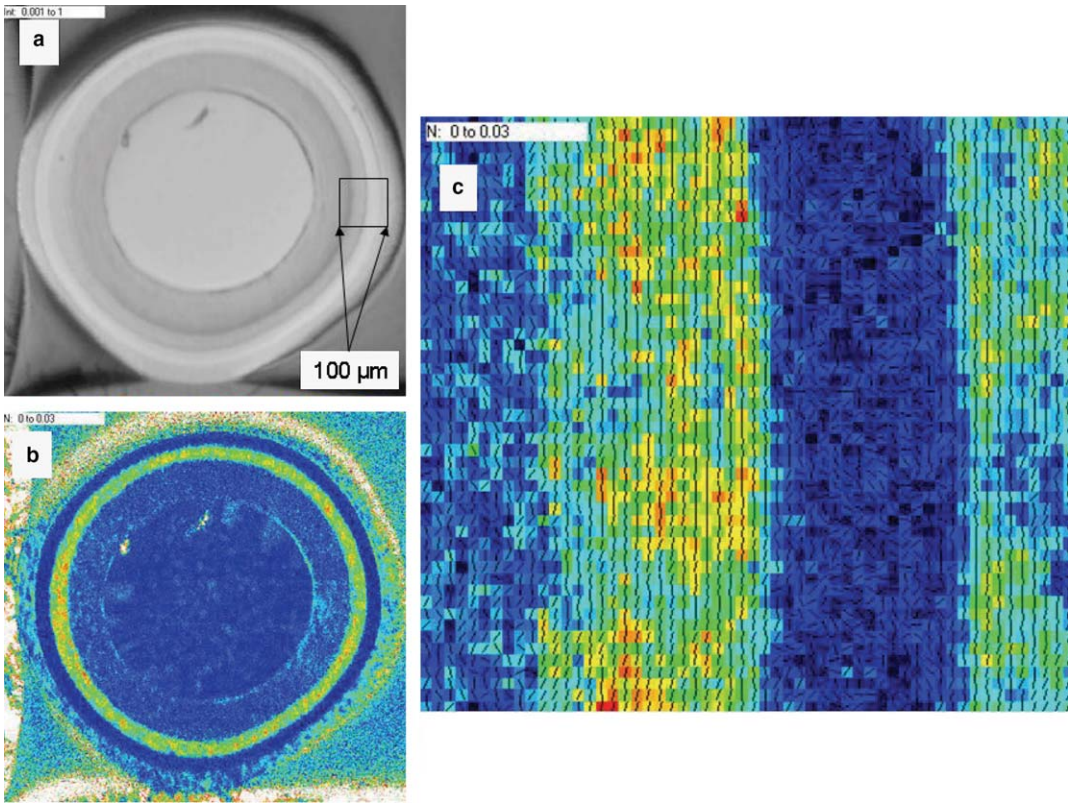

Fig. 4. 2-MGEM data taken on a German TRISO Fuel particle. (a) Intensity (log scale); (b) diattenuation (full particle, 0–0.03), (c) diattenuation, boxed region with the principal axis superimposed. See Fig. 2 for the scale.

the entire circumference of the particle image. The diattenuation plot (Fig. 4(b)) corresponds to the intensity plot point-for-point. Other parameters (such as the retardation and circular diattenuation) are recorded but are not as revealing as the diattenuation and direction of the fast axis. Fig. 4(c) shows a blow-up of the diattenuation of the regions indicated by the square in Fig. 4(a).

5. Concluding remarks

From Figs. 2–4 several conclusions can be drawn:

(1) The IPyC does indeed show considerable diattenuation, and this is a function of growth conditions. For IPyCs that have high diattenuation, the direction of the principal axis is predictably nearly along the tangent of the layer. This indicates that the graphine layers are predominantly aligned perpendicular to the growth direction, as would be expected. For particles that show much less diattenuation (Fig. 3(b) and (c)), this alignment of the direction of the principal axis is not as predictable, though there is a consistency within individual regions of relatively high diattenuation.
(2) Even for highly anisotropic IPyC layers, the diattenuation is not uniform (see Figs. 3(a) and 4(c)), nor is there any obvious variation from the inside boundary to the outside boundary.
(3) The SiC layer shows very little diattenuation, as expected.
(4) Some parts of some buffer layers show diattenuation, but it is considerably smaller than the diattenuation of the IPyC.
(5) The OPyC seen in Fig. 4 does show some diattenuation, and the value is ~1/2 that of the IPyC.

Acknowledgements

Research was sponsored by the Office of Nuclear Energy, Science and Technology and Oak Ridge

National Laboratory, managed by UT-Battelle, LLC, for the US Department of Energy under contract No. DE-ACO5-00OR22725.

References

[1] A. Borghesi, G. Guizzetti, in: E.D. Palik (Ed.), Handbook of Optical Constants of Solids II, Academic Press, 1991, p. 449.
[2] A.B. Djurisic, E.H. Li, J. Appl. Phys. 85 (1999) 7404.
[3] G.E. Jellison Jr., F.A. Modine, Appl. Opt. 36 (1997) 8184.
[4] G.E. Jellison Jr., F.A. Modine, Appl. Opt. 36 (1997) 8190.
[5] G.E. Jellison Jr., C.O. Griffiths, D.E. Holcomb, C.M. Rouleau, Appl. Opt. 41 (2002) 6555.
[6] G.E. Jellison Jr., J.D. Hunn, C.M. Rouleau, Appl. Opt., accepted for publication.
[7] G.E. Jellison Jr., F.A. Modine, L.A. Boatner, Opt. Lett. 22 (1997) 1808.